EUROPEAN COMMISSION
JOINT RESEARCH CENTRE
ENVIRONMENT INSTITUTE

Environmental Modelling Task Force

Influence of NOx/VOC emission-reduction on ozone levels in the Mediterranean area

C. Cuvelier, P. Thunis

Introduction

The EU-wide abatement strategy, as described in the *Ozone Position Paper*, focusses on the large scale ozone levels (cf *D. Simpson, 1998, The scientific basis of NOx protocols and the EU ozone control strategy, paper at EUROTRAC-2*). It is based on model calculations with a resolution of 150 km and does not address peaks of spatial dimensions below this size. It is known that on the regional and urban scale peaks can occur, superimposed on the larger scale background. The target values and the LTO's also apply to these peaks. It is, however, not practical to attempt to devise a detailed EU strategy for such peaks, since these may occur under quite different conditions, and the best way to combat such peaks may depend on the local situation. Because of this, it is left to the Member States to choose the best approach to abate local ozone levels. It is, however, important to investigate how large measures affect the local situation.

In this contribution to the study of the strategy for the regional (meso-) scale, we will concentrate on the situation in the Mediterranean area with a case study from the Burriana area (near Valencia, Spain).

Meteorology and air pollution in the Mediterranean

For general reference, see *Millan et al, 1992, MECAPIP report; Millan et al, 1996, Atmos Env. 30, 1909-1924; Millan, Salvador, Mantilla, Kallos, 1997, J. Geophys. Res, 102, 8811-8823; Millan, 1998, Ozone Position Paper, annex C;* and *Kallos, paper presented at EUROTRAC-2.*

There is experimental evidence for chronic air pollution problems in Southern Europe, e.g. on the Spanish east coast the ozone threshold level of the EC directive 92/72/CEE for damages to vegetation (65 μg/m^3 as a 24 hours average) is exceeded for more than 6 months of the year, the one for human health (110 μg/m^3, 8 hour average) for at least four months, and the one for information to the population (180 μg/m^3, hourly average) can also be exceeded frequently from April to August. This situation is the norm for coastal regions surrounding the western Mediterranean Basin.

Convection and recirculation seem to predominate in the western Mediterranean area, possibly leading to a build-up and cooking of pollutants. Horizontal advection seems to predominate in the eastern Mediterranean area, in a way that air pollution from urban areas within the region is transported as plumes over the sea.

Within the synoptic meteorological patterns, mesoscale patterns develop, with marked diurnal cycles and spatial scales of tens of kilometres. They are induced by sea-land and upslope-downslope winds, and are typical for Southern Europe with its complex coastal and orographic features and high solar radiation. The concepts “downwind and upwind of sources loose their straightforward meaning and must be reconsidered in the light of these mesoscale recirculations.

Computational results

The computational results are obtained using the EI/EMTF integrated modelling system consisting of a meteorological model, a tracer transport code and one of the two gas-phase chemistry modules LCC or RACM. The combined meteorological/transport model is the Topographic Vorticity Mesoscale model TVM (cf. *Schayes et al, 1996, J. of Appl. Meteorology, 35, 1815-1823).* The model LCC (cf. *Lurman, Carter, Coyner, 1987, EPA report No. 600/3-87/014A*) simulates 106 chemical gas-phase reactions for 44 chemical species. The Regional Atmospheric Chemistry Mechanism RACM (cf. *Stockwell et al, 1997, J. Geophys. Res. 102, D22, 25847-25879*) treats 237 reaction equations for 65 species.

Figure 1

The computational domain and topography employed in the simulations for the Burriana site are shown in Figure 1. In order to increase the accuracy in the region between Burriana and Valbona, a non-uniform mesh has been chosen. Its resolution ranges from 1 by 1 km2 in a rectangle of 42 km west-east and 35 km south-north extent between Burriana and Valbona to progressively reach a 5 by 5 km2 resolution at the edges of the domain. The outer perimeter in Figure 1 delimits the total area in which the meteorological model is run. The domain is covered by a (72 x 58) grid system. The same horizontal domain is used for both the meteorology and the photochemistry calculations. In the vertical direction a terrain-following σ-coordinate system is defined. For meteorological computations, 25 levels were selected reaching an altitude of approximately 12 km with a non-uniform spacing ranging from 30 m to 1 km while for chemistry computations only the 14 lowest layers were used.
The contour lines in Figure 1 indicate terrain elevation at intervals of 100 m.

Figure 2

Here the diurnal results for the formation and depletion of ozone of the 3-dimensional simulations are shown in a vertical plane perpendicular to the coast intersecting the sites of Burriana and Cirat.
During the night the formation of the drainage flow (the accumulation of a stable air mass at the bottom of the valleys and over the coastal plains) generates an offshore flow. In the morning and due to the increasing temperature of the land, the draining air mass becomes blocked at some distance from the coast. Due to further heating of the land, the sea-breeze is fully developed by mid-afternoon. The onshore and inland air flow continues into the evening hours, with wind speeds decreasing and becoming stagnant by midnight.
Concerning the chemistry the computational results show the following: At night, when photochemistry is not active, anthropogenic NO emissions near the coast lead to a strong depletion of O3 which lowers its concentration to near-zero values. Under the

influence of the land breeze this low-ozone air mass is transported over the sea offshore, where further depletion of ozone takes place. Note that the strong atmospheric stability at these times creates a highly variable vertical profile for ozone concentrations near the shore. Values at surface are close to zero while at a few hundred meters altitude, they reach approximately 60 ppb.

From the early morning on the calculations show the entrance of the sea breeze taking with it the air mass from the sea. Due to the influence of the photochemistry, the emissions of NOx and anthropogenic VOCs, a production of ozone takes place. These ozone concentrations can reach relatively high values in land (up to 120 ppb in Cirat). As a consequence of the reverse flow on top of the sea-breeze, this ozone-rich air mass is transported to higher levels, called the reservoir layer.

Figure 3

This figure shows the evolution of the ozone concentration field (simulated with TVM/RACM) for six different instants of time of June 12th. The corresponding TVM wind directions are not shown in detail but only schematically by arrows.

At 04:00 LST, the nocturnal cooling of the inland ground surfaces has led to the formation of down-slope flows on each individual hill or mountain within the domain. These slope flows have progressively filled valleys with cold air and the resulting pressure gradient has led to the development of valley flows. By the same effect of differential cooling between water and inland surfaces, a land breeze is at that time fully developed and directly influences coastal locations such as Burriana, Sagunto or Castellon. The meteorology (temperature, wind speed and direction) is generally well reproduced for all stations except at Cirat for which the underestimation in wind speed is probably due to the lack of resolution in this area.

At coastal sites, the high NOx emissions (VOC limited regime) lead to very low ozone values. At Onda, which is located a few kilometers inland, the ozone levels much depend on the wind direction and slight changes in the latter can produce low ozone values. Hence, the ozone night-time evolution at this station exhibits a very chaotic behaviour. For more inland stations like Cirat or Valbona, night time ozone values never drop below 20 or 30 ppb. These values are lower than the background value (50 ppb) and indicate some ozone depletion which is either due to local emissions or to transport of polluted air from the Western part of the domain.

At sunrise, land surface starts to warm up and pressure gradients reverse. Up-slope flows directly form simultaneously with the onset of the sea-breeze. As a consequence, the flow is directed onshore over the whole domain at approximately the same time. This onshore flow carries with it the night-time pollutants which starts entering the classical chain of photochemical reactions. These reactions are at that time very efficient since over the sea, the mixing layer is very limited. When these pollutants reach the coast, a sudden rise in ozone concentrations is observed. This is the case at coastal stations like Burriana where after the passage of the breeze front, ozone concentrations drop down. After the passage of the breeze front, ozone values generally do not exceed the background value since large emissions are continuously active (persistence of the VOC limited regime).

At mid-afternoon, while photo-chemistry is acting on the newly emitted compounds, the cloud of maximum ozone concentrations corresponding to the transformation of night-time emissions is pushed further inland to the North-West. Locations such as Cirat experience a sharp rise in ozone concentration at 16:00 LST, whereas at Valbona the sea-breeze ozone peak only arrives at 18:00 LST. At this location, two clear peaks are observed, the first one probably due to local photochemistry, while the second is the result of the sea-breeze arrival.

After sunset, photochemical reactions are inhibited and emissions are again constrained in a very shallow layer that favours ozone destruction. This is the case at nearly every inland station. At Cirat, the day-time peak is relatively well reproduced.

Figure 4

In this figure we show a NOx-AVOC emission reduction isopleth for AOT40 and AOT60 values for Burriana and Cirat. On the horizontal axis the NOx emissions are given as a fraction of the base-case; the vertical axis gives the fraction of the base-case AVOC emissions. The point (1.,1.) corresponds to the base-case emission inventory. The point REF corresponds to the “Reference-Reduction” (i.e. 23% NOx, 25% AVOC reduction); the point MFR to the “Most-Feasible-Reduction” (i.e. 59% NOx, 53% AVOC reduction). The diurnal values for AOT40 and AOT60 (in units: ppm.hr) are multiplied by 90 to correspond with the 3 months period in the definition of AOT40. AOT40 values for Burriana range from approximately 7.0 to 19.0. The AOT60 value for Burriana is equal to zero, because the ozone levels never exceed 60 ppb. In Cirat the AOT60 ranges from 12.5 to 37.0. We conclude that at Burriana the REF and the MFR reductions do increase the AOT40 values. In Cirat the REF and MFR reductions have almost no influence on the values of AOT40, and do decrease the values of AOT60.

We note that the AOT values may be overestimated due to the multiplication by 90 of the diurnal values.

Figure 5

The top figure shows the AOT40 values in the 3-dimensional case at ground level. The bottom figure depicts the difference of the MFR reduction case with the base-case.

Absolute values range from 10 ppm.hr (blue area) to 40 ppm.hr (red area). The impact of the MFR reduction is positive but small in the yellow part (increasing values for AOT40), and negative (i.e. lower values of AOT40) in the blue part of the picture.

Figure 6

Same as for Figure 5, but for AOT60 values. AOT absolute values are 0. in the purple part, and take maximum values of 20 ppm.hr in the red part. The impact of the MFR reduction is 0. in the yellow area, and negative (decreasing AOT60) in the blue area.

Figure 1

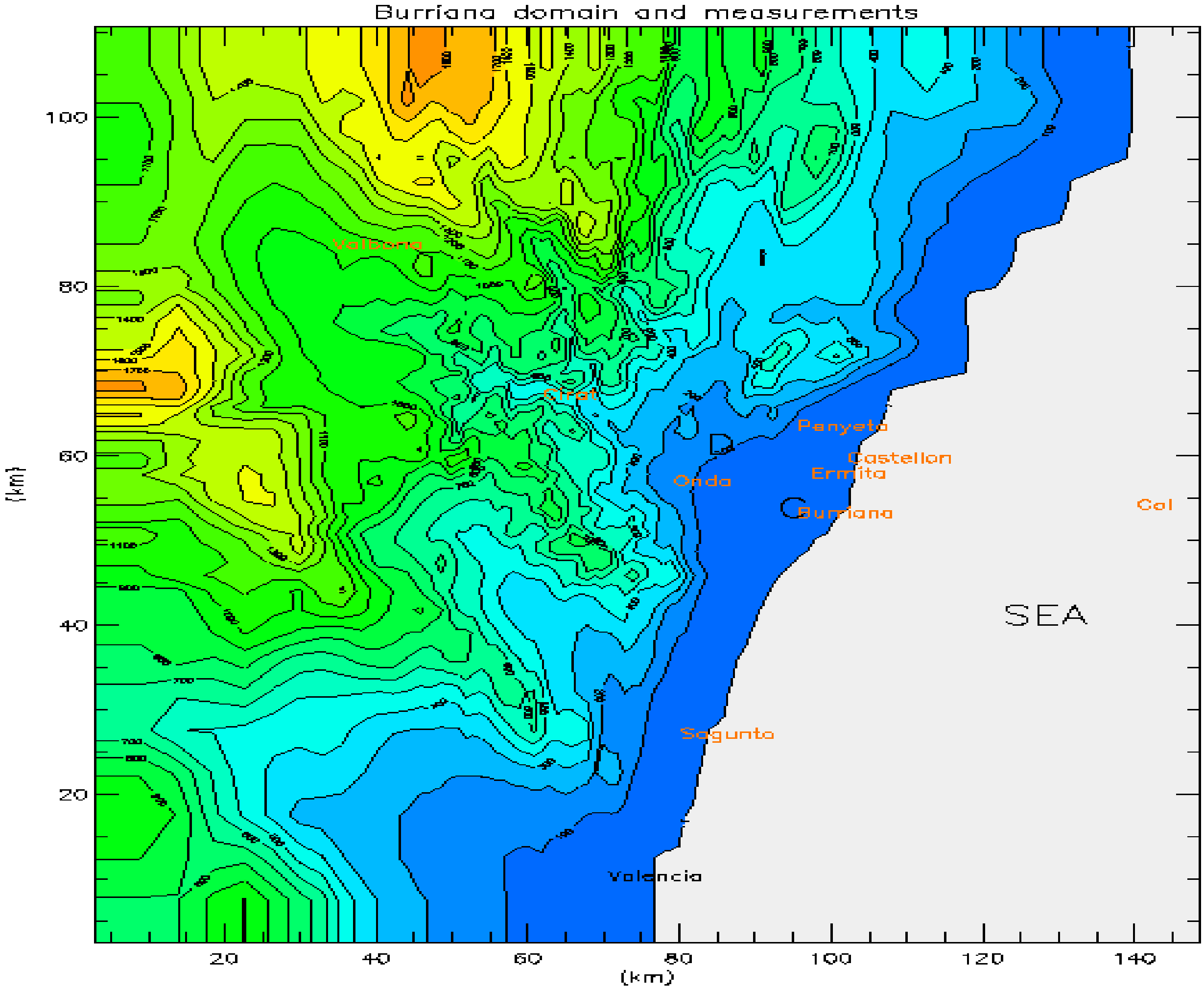
Burriana domain and measurements
Valbona
Cirat
Penyeta
Castellon
Ermita
Onda
D
C
Burriana
Col
SEA
Sagunto
Valencia
100
80
60
40
20
(km)
20
40
60
80
100
120
140
(km)

Figure 2

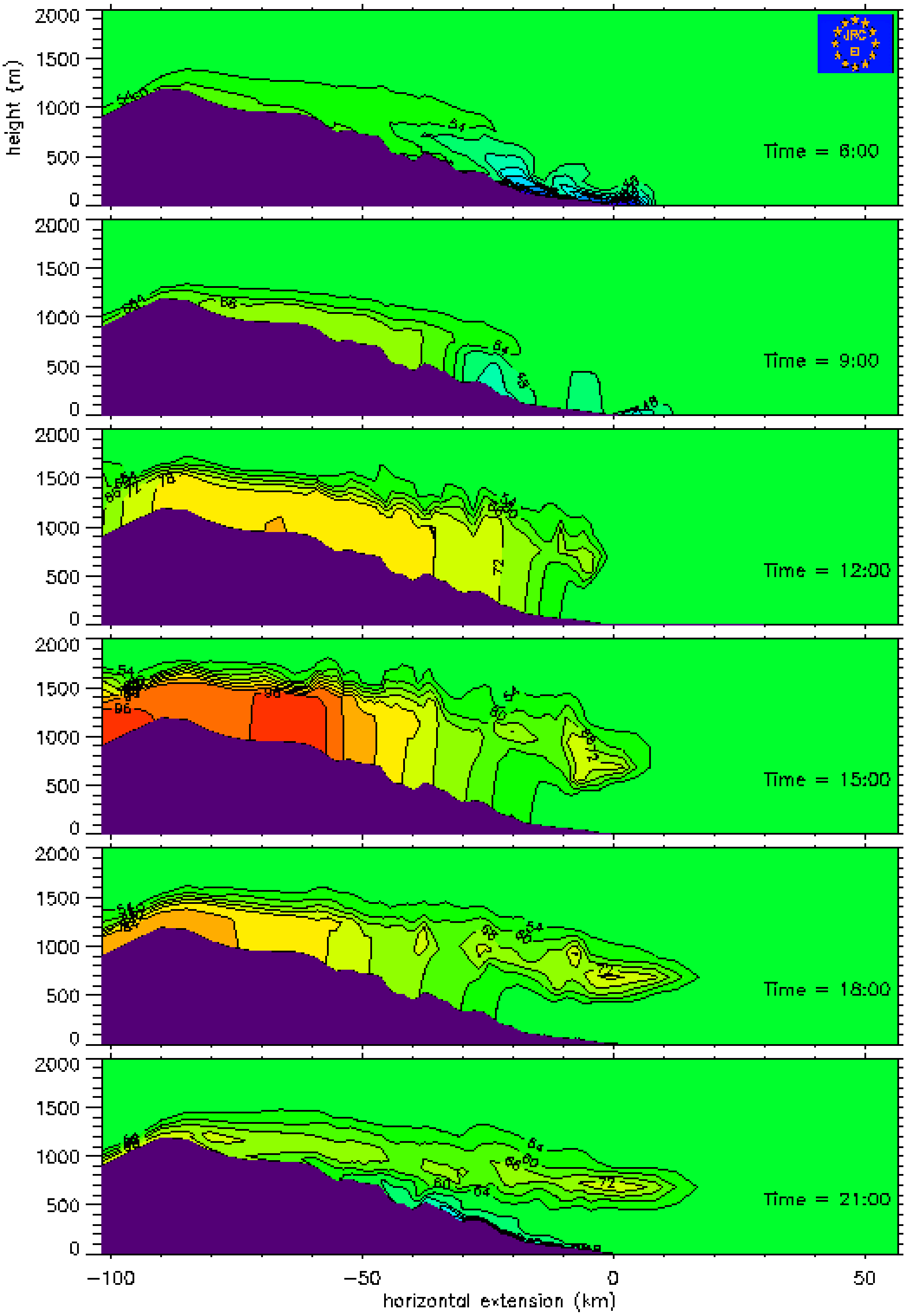
height (m)
2000
1500
1000
500
0
Time = 6:00
Time = 9:00
Time = 12:00
Time = 15:00
Time = 18:00
Time = 21:00
JRC
-100
-50
0
50
horizontal extension (km)
54
66
72
78
96
48

Figure 3

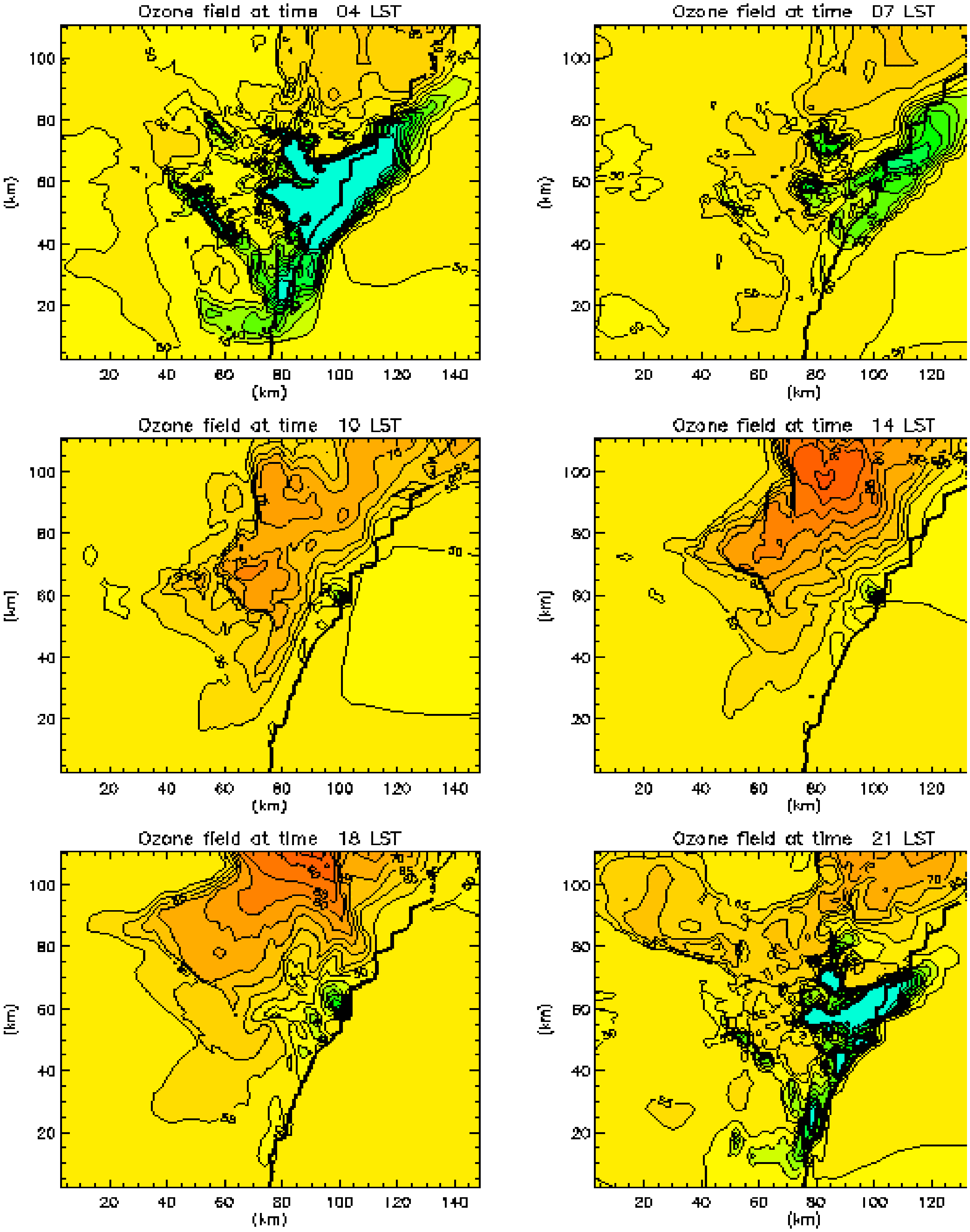
Ozone field at time 04 LST
Ozone field at time 07 LST
Ozone field at time 10 LST
Ozone field at time 14 LST
Ozone field at time 18 LST
Ozone field at time 21 LST
(km)
(km)
20
40
60
80
100
120
140

Figure 4

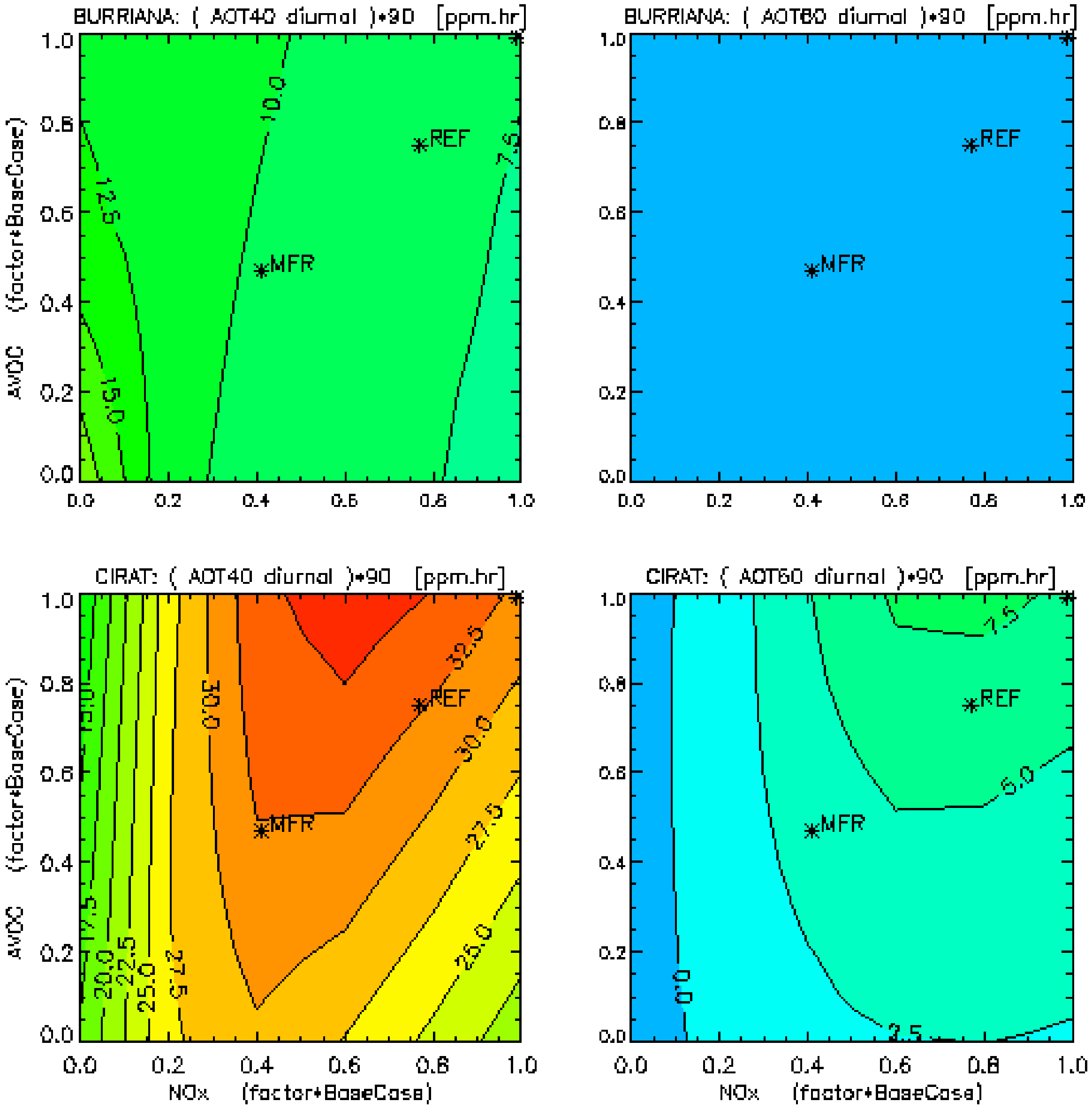
BURRIANA: (AOT40 diurnal)*90 [ppm.hr]
BURRIANA: (AOT60 diurnal)*90 [ppm.hr]
CIRAT: (AOT40 diurnal)*90 [ppm.hr]
CIRAT: (AOT60 diurnal)*90 [ppm.hr]
AVOC (factor*BaseCase)
NOx (factor*BaseCase)
0.0
0.2
0.4
0.6
0.8
1.0
REF
MFR
7.5
10.0
12.5
15.0
17.5
20.0
22.5
25.0
27.5
30.0
32.5
0.0
2.5
5.0
7.5

Figure 5

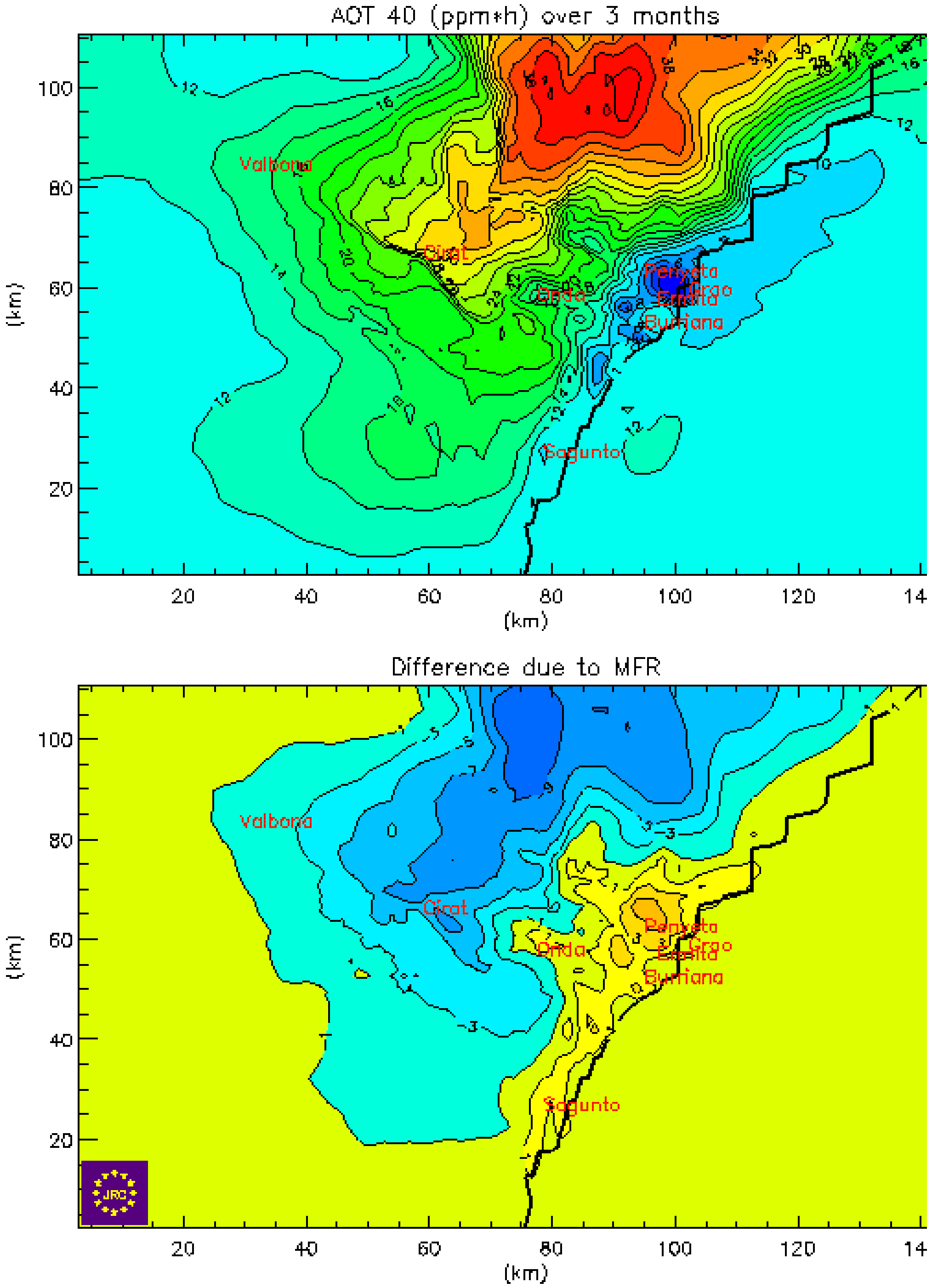
AOT 40 (ppm*h) over 3 months
Difference due to MFR
(km)
20
40
60
80
100
120
14
Valbona
Cirat
Onda
Penyeta
Grao
Estrita
Burriana
Sagunto
JRC

Figure 6

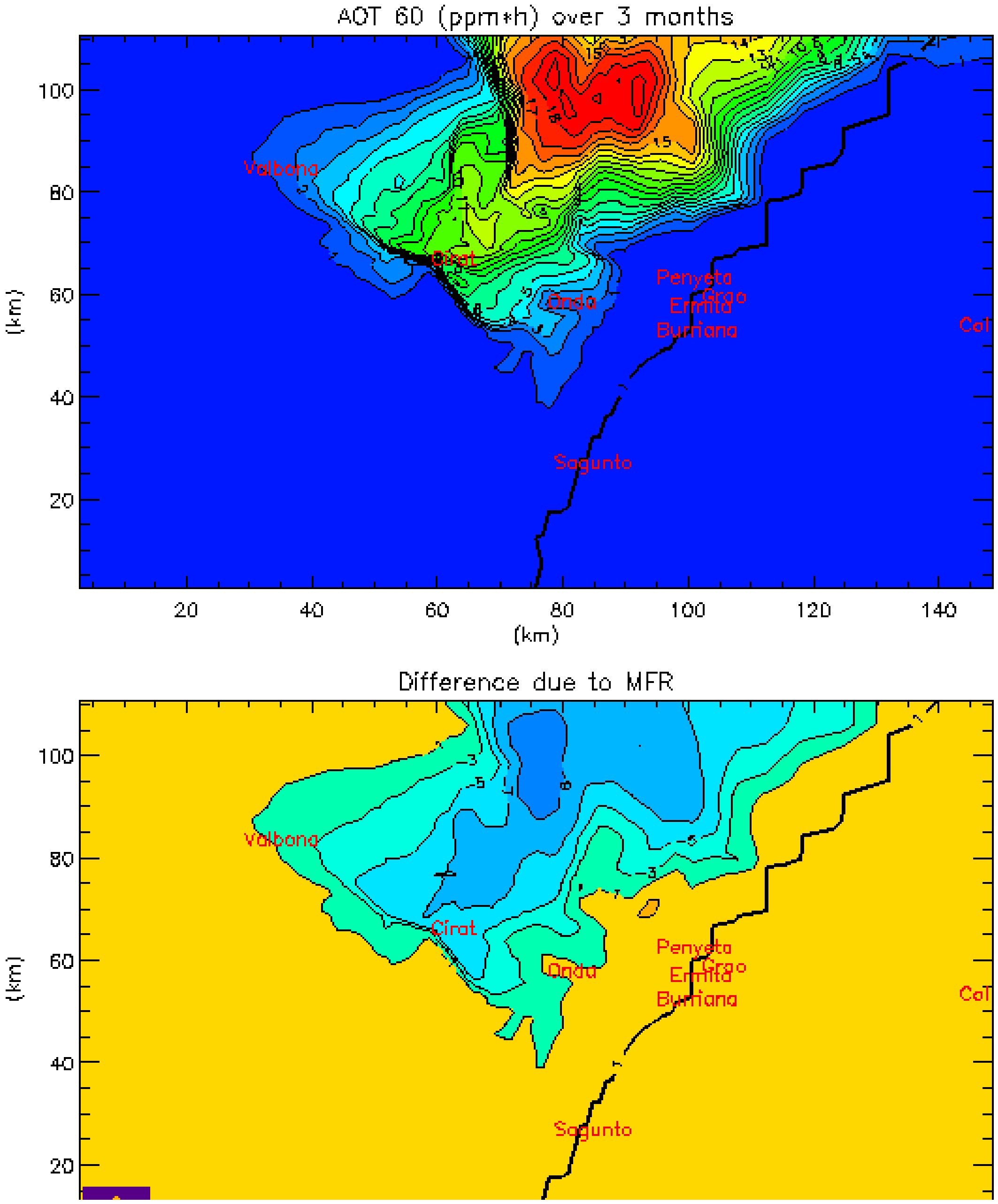
AOT 60 (ppm*h) over 3 months
Difference due to MFR
(km)
100
80
60
40
20
20
40
60
80
100
120
140
Valbona
Cirat
Penyeta
Grao
Ermita
Onda
Burriana
Col
Sagunto